10th World Congress on Structural and Multidisciplinary Optimization
May 19 -24, 2013, Orlando, Florida, USA

Multidisciplinary Level Set Topology Optimization of the Internal Structure of an Aircraft Wing

Peter D Dunning[1], Christopher J. Brampton[2], H. Alicia Kim[2]

[1] National Institute of Aerospace, Hampton, Virginia, United States of America, VA 23666, peter.dunning@nianet.org
[2] Department of Mechanical Engineering, University of Bath, Bath, United Kingdom, BA2 7AY

1. Abstract
A method is introduced for optimizing the internal structure of a wing that explicitly includes the effect of the coupled aerodynamic loading. This is achieved though a multidisciplinary analysis of the system and a coupled sensitivity analysis. The design problem is to minimize the compliance of the structure subject to a constraint that lift must be greater than or equal to weight. The level set based method is used to optimize the three-dimensional topology of the wing internal structure. A new technique is introduced to handle the constraint within the level set optimization method. This involves approximating the constraint to be linear and then estimating the change using numerical integration. The method performs well, as the optimization improves the structural performance and satisfies the constraint. The optimized design of an example wing was remarkably different to a conventional wing structure.

2. Keywords: Topology optimization, Level set method, Multidisciplinary optimization, Wing structure.

3. Introduction
The primary load-carrying component of modern aircraft wings is a wing box composed of spars and skin stiffened by ribs. The spar-skin-rib configuration has dominated wing design for a number of decades and exploration of alternative configurations has been limited. One reason for this may be attributed to the complex coupling of aerodynamics and structures. A wing is a classic example of a multidisciplinary problem where aerodynamic and structural design requirements are conflicting and yet intimately related.
Topology optimization has been used as a tool for exploring new aircraft wing designs. The initial attempts simply computed the aerodynamic load distributions on the initial wing design and then used those loads to optimize the internal structure of the wing, without updating the aerodynamics loads. Balabanov and Haftka [1] represented the internal structure of a wing as a truss and optimization was applied to the cross-sectional area of the ground structure of interconnected truss elements. Eschenauer and Olhoff [2] represented the internal wing as a continuum and used their bubble method to optimize for a set of loadings obtained from pull-up maneuvers and tank pressures. Maute and Allen [3] applied the SIMP method to a 2D continuum of a flat plate wing with coupling to aerodynamics. The optimum solutions were topologies of stiffener distributions that were very different from an orthogonal spar-rib configuration. This work also indicated that the coupling between aerodynamics and structures fundamentally influences the optimum solution and is an important consideration. As SIMP has become very popular, efforts have been seen in applying SIMP to aero-structural and aeroelastic wing optimization [4,5]. Some recent work extends the optimization method to consider material anisotropy and topology simultaneously [6]. Whilst there has been a level of success in achieving favorable performance characteristics, it became apparent that the convergence could be slow and challenging. In addition, it was not always straightforward to reduce to the optimum solutions to a 0/1 design where the structure was clearly defined. The solutions often contained large "grey" regions of intermediate material properties, which do not lend themselves easily to a topological equivalence. Thus, the challenges lie in the interpretation of the solution to a manufacturable design. Alternative methods have been applied to address this challenge.
Kobayashi *et al* [7] apply their cellular division method to design the wing box of a fighter aircraft. This is a biologically inspired method that does not require sensitivities, hence can be applied to a wide range of problems. A typical criticism of such methods is that the convergence can be slow, as the search is not directed by sensitivities. Another topology optimization approach that has been attracting a great deal of attention is based on the level set method [8-10]. The level set method was developed to track fronts in 2D or 3D. It defines the boundaries of a structure by an implicit function and naturally allows boundary merging and splitting in a continuous manner. The level set method always defines clear boundaries and therefore avoids solutions with grey area and intermediate material properties. The level set method has been applied to wing optimization for an aeroelastic effect of aileron reversal and provided good convergence with clearly defined structures [11]. Noting that much of the topology optimization has been applied to a 2D domain, Brampton *et al* [12] applied

level set based topology optimization to a simple 3D wing box with coupled aerodynamic and structural analysis. This paper considered a simple cruise condition for a non-swept linearly tapered wing. The preliminary results showed that the 3D topological optimum solutions are very different from the 2D solutions and also the conventional spar-rib configuration. However, the results showed that optimization does not necessarily reduce the overall aerodynamic loading.

This paper presents a strategy for optimizing the internal structure of a wing that explicitly includes the effect of the coupled aerodynamic loading. This was achieved though a multidisciplinary analysis of the system and a coupled sensitivity analysis. To obtain a solution with clearly boundaries, the level set based method was used to optimize the three-dimensional topology of the wing internal structure. A new technique for handling constraints in the level set method is also introduced.

4. Problem formulation

The problem studied in this paper was to minimize the compliance of the internal wing structure. The loading on the structure was the lift force generated by a single steady-state flight condition. The lift loads were dependent on the deformed shape of the wing, which in turn was dependent on the applied loading. Therefore, the structure was part of a coupled, multidisciplinary system. A constraint was added that the total lift generated by the wing must be able to support the aircraft weight. The problem can be stated as:

$$\begin{aligned} &\text{Minimize}: \; C(u) = f^T u \\ &\text{Subject to}: \; L(u) \geq W_c + W_b \\ &\qquad\qquad Ku = f_c + Qu \end{aligned} \tag{1}$$

where u is the deformed shape of the wing, $C(u)$ is the total compliance of the wing, f is the total load vector ($f = f_c + Qu$), K is the structural stiffness matrix, Q is the aerodynamic stiffness matrix, f_c is a constant load vector resulting from a rigid wing set at a specified angle of attack, $L(u)$ is the total lift generated by the deformed wing shape, W_b is the weight of the wing box that can change during the optimization and W_c is the remaining "fixed" weight of the aircraft. The second constraint in Eq.(1) is the static equilibrium of the aero-structural system. Note that Q is constant for a constant wing planform and flight conditions (velocity, air density and Mach number). The total lift force acting on the wing was simply computed by summing the rigid and deformed wing shape contributions:

$$L(u) = z^T \left(f_c + Qu \right) \tag{2}$$

where z is a unit column vector (all entries are 1).

4.1. Shape sensitivity analysis

To obtain the shape sensitivities for the objective and constraints in Eq.(1) we follow the method of Allaire *et al* [1] and account for the influence of the aerodynamic stiffness on the structural response. The method is briefly outlined here for a generic boundary integral function that is assumed smooth and differentiable:

$$J(u) = \int_\Gamma j(u)\, d\Gamma \tag{3}$$

where Γ is the total structure boundary and $j(u)$ is a generic function. A Lagrangian is formulated for Eq.(3) and the coupled aero-structural system:

$$\Lambda(u) = \int_\Gamma j(v)\, d\Gamma + \int_{\Omega_S} E_{ijkl} \varepsilon_{ij}(v)\; \varepsilon_{ij}(p)\, d\Omega_S - \int_\Gamma \left(f_{c,j} + Q_{ij} v_i \right) p_j\, d\Gamma \tag{4}$$

where Ω_S is the domain of the structure, v is any kinematically permissible displacement vector, E is the material property tensor, $\varepsilon(u)$ is the strain tensor and p is a Lagrange multiplier for the aero-structural equilibrium equation. By considering the stationary points of the Lagrangian, Eq.(4), the shape sensitivity and adjoint state for the function $J(u)$ can be found:

$$J'(u) = \int_{\Gamma_0} E_{ijkl} \varepsilon(u)_{ij} \varepsilon(p)_{kl} V_n\, d\Gamma_0 \tag{5}$$

$$\int_{\Omega_S} E_{ijkl} \varepsilon(p)_{ij} \varepsilon(v)_{kl}\, d\Omega_S = \int_\Gamma \left(\partial j(u) / \partial u \right) v\, d\Gamma + \int_\Gamma Q_{ij} p_j v_i\, d\Gamma \tag{6}$$

where Eq.(5) is the shape sensitivity, Eq.(6) is the adjoint equation, Γ_0 is part of the structure boundary that is not

subject to loads or boundary conditions, V_n is a velocity function defined normal to the boundary, such that a positive velocity moves the boundary inwards

Equations (5) and (6) were used to derived shape sensitivities for the objective and constraints in Eq.(1). The compliance objective from Eq.(1) can be written in a continuous form:

$$C(u) = \int_{\Gamma} \left(Q_{ij} u_i u_j + f_c \cdot u \right) d\Gamma \tag{7}$$

Using the result of Eq.(5) and substituting: $j(u) = (Q_{ij}u_iu_j + f_c \cdot u)$ into Eq.(6), after some further manipulation, the shape sensitivity for the compliance objective is:

$$C'(u) = \int_{\Gamma_0} \left[E_{ijkl}\varepsilon(u)_{ij}\varepsilon(p_c)_{kl} - E_{ijkl}\varepsilon(u)_{ij}\varepsilon(u)_{kl} \right] V_n \, d\Gamma_0 \tag{8}$$

and p_c is the solution to the following adjoint equation:

$$\int_{\Omega_S} E_{ijkl}\varepsilon(p_c)_{ij}\varepsilon(v)_{kl} \, d\Omega_S = 2\int_{\Gamma} f \cdot v d\Gamma + \int_{\Gamma} Q_{ij} p_{c,j} v_i d\Gamma \tag{9}$$

and f is the total load. When solved using numerical methods, the adjoint equation, Eq. (9), can be written in discrete matrix form:

$$Kp_c = Q^T p_c + 2f \tag{10}$$

Assuming that the wing box is made from a uniform density material, the weight is equal to the total volume multiplied by the material density and gravity. Thus, the sensitivity of the wing box weight is simply equal to the sensitivity for volume multiplied by material density and gravity:

$$W' = \int_{\Gamma_0} -\rho g V_n d\Gamma_0 \tag{11}$$

where ρ is the material density and g is acceleration due to gravity. It remains to derive the sensitivity for the lift part of the constraint. The lift function, Eq.(2), can be written in a continuous form:

$$L(u) = \int_{\Gamma} \left(f_{c,j} + Q_{ij} u_i \right) z_j d\Gamma \tag{12}$$

Again, using the result of Eq.(5) and substituting: $j(u) = (f_{c,j} + Q_{ij}u_i)z_j$ into Eq.(6), the shape sensitivity for the lift function is:

$$L'(u) = \int_{\Gamma_0} E_{ijkl}\varepsilon(u)_{ij}\varepsilon(p_l)_{kl} V_n d\Gamma_0 \tag{13}$$

where p_l is the solution to the adjoint equation:

$$\int_{\Omega_S} E_{ijkl}\varepsilon(p_l)_{ij}\varepsilon(v)_{kl} \, d\Omega_S = \int_{\Gamma} Q_{ij} z_j v_i d\Gamma + \int_{\Gamma} Q_{ij} p_{l,j} v_i d\Gamma \tag{14}$$

The adjoint equation for the lift can also be written in discrete matrix form:

$$Kp_l = Q^T \left(p_l + z \right) \tag{15}$$

Note that in deriving Eq.(10) and Eq.(15) it was assumed that the structural stiffness matrix, K was symmetric, but that the aerodynamic stiffness matrix, Q was not.

4.2. Constraint handling

The first constraint of the optimization problem shown in Eq.(1) was added to the objective using a Lagrange multiplier to form an unconstrained problem:

$$\text{Minimize}: \; F(u) = f^T u + \lambda \left[W_c + W_b - L(u) \right] \tag{16}$$

where λ is a Lagrange multiplier. It was assumed that the equilibrium constraint was satisfied when solving for the deformed shape of the wing during an iteration of the optimization. The shape sensitivity for the unconstrained problem can be formulated by adding the shape sensitivities for the separate functions that were derived in Eqs.(8,11,13):

$$F'(u) = \int_{\Gamma_0} \left[E_{ijkl}\varepsilon(u)_{ij}\varepsilon(p_c)_{kl} - E_{ijkl}\varepsilon(u)_{ij}\varepsilon(u)_{kl} - \lambda \left(\rho g + E_{ijkl}\varepsilon(u)_{ij}\varepsilon(p_l)_{kl} \right) \right] V_n d\Gamma_0 \tag{17}$$

5. Level set based optimization

The multidisciplinary optimization problem formulated in Section 4 was solved using the level set based topology optimization method [8-10]. The method is briefly outlined followed by a few details of the implementation and a more detailed discussion of the technique introduced to compute the Lagrange multiplier. First, the boundary of the structure is defined as the zero level set of an implicit function:

$$\begin{cases} \phi(x) \geq 0, x \in \Omega_s \\ \phi(x) = 0, x \in \Gamma \\ \phi(x) < 0, x \notin \Omega_s \end{cases} \tag{18}$$

where $\phi(x)$ is the implicit function and $x \in \Omega$, where Ω is the design domain containing the structure, $\Omega_S \subset \Omega$. The implicit description of the structure allows the boundary to break and merge naturally. This allows for topological changes to the structure to occur during optimization. The implicit function can be updated under a velocity field over time by iteratively solving a Hamilton-Jacobi type equation:

$$\frac{\partial \phi(x)}{\partial t} + \nabla \phi(x,t) \frac{dx}{dt} = 0 \tag{19}$$

where t is a fictitious time domain. Equation (19) can be discretized and rearranged to provide a convenient update formula for optimization:

$$\phi_i^{k+1} = \phi_i^k - \Delta t \left| \nabla \phi_i^k \right| V_{n,i} \tag{20}$$

where i is a discrete point on the boundary of the structure, k is the current iteration number and Δt is a discrete time step. The velocity function should be defined such that the movement of the boundary improves the objective. This can be achieved using shape sensitivity analysis and a descent method analogy. For the unconstrained problem defined by Eq.(16) the shape sensitivity is defined by Eq.(17). If the velocity function is defined as the negative of the value in the square brackets in Eq.(17), then the shape sensitivity for the objective will be negative everywhere on the boundary. This ensures that the objective will reduce when the structure is updated using Eq.(20). Thus, the velocity function used in this work was defined as:

$$V_n = \lambda \left(\rho g + E_{ijkl} \varepsilon(u)_{ij} \varepsilon(p_l)_{kl} \right) - E_{ijkl} \varepsilon(u)_{ij} \varepsilon(p_c)_{kl} + E_{ijkl} \varepsilon(u)_{ij} \varepsilon(u)_{kl} \tag{21}$$

The shape sensitivity in Eq.(17) only applies to the part of the boundary that is free from loading and boundary conditions, Γ_0. Thus, the velocity function in Eq.(21) also applies only to the free part of the boundary. For practical reasons, the remaining part of the boundary is fixed during the optimization by setting the velocity function to zero.

5.1. Implementation

A 3D level set method was used to optimize the internal structure of the wing. The design domain was divided into equal sized cubes and the implicit function was discretized at the vertices. The same grid was also used for the finite element mesh used for the structural analysis. Details of the approach to solve the multidisciplinary aero-structural equilibrium equation are included below in Section 6. The implicit function was initialized as a signed distance function, where the value of the implicit function indicated the distance to the boundary and the sign was defined by Eq.(18).

For efficiency the finite element mesh remained fixed during optimization. Therefore, some elements can be cut by the structure boundary leading to a discontinuity in material properties within the element. Discontinuous elements were treated using a volume-fraction weighted approximation for the element stiffness matrix [13]:

$$K_{e,i} = (\beta_i / \beta) K_e \tag{22}$$

where $K_{e,i}$ is the stiffness matrix of a cut element, K_e is the stiffness matrix of a continuous tri-linear element with volume β and β_i is the volume of element i that lies inside the structure. Once the primary and adjoint equations have been solved, sensitivity values are computed at element Gauss points and interpolated at the boundary using a weighted least squares method [14]. The sensitivity values were used to compute velocity function values at points along the boundary using Eq.(21).

The velocity function, Eq.(21) is defined only at points on the structure boundary. However, discrete velocity values, $V_{n,i}$ are required at all grid points to update the level set function using Eq.(20). This was achieved by extrapolating velocities away from the boundary using a velocity extension technique that helps maintain the signed distance property of the implicit function [15], which is important for the stability of the level set method. For efficiency, the velocity extension computation was limited to a narrow band region around the boundary and

the update was limited to this region [15]. The narrow band was defined as six grid lengths either side of the initial boundary. When the boundary approached the edge of the narrow band region, the band was redefined from the current boundary. However, the narrow band method can lead to implicit functions that are too steep or shallow, which can reduce the accuracy and stability of the level set method. Thus, the implicit function was re-initialized as a signed distance function using the fast marching method [15] whenever the narrow band was redefined and also periodically to maintain accuracy and stability. The upwind finite difference method [15] with a higher order Weighted Essentially Non-Oscillatory scheme [16] was used for the gradient calculation of the implicit function. Finally, the time step was defined by the Courant–Friedrichs–Lewy condition for stability:

$$\Delta t = h / 2\left|V_{n,i}\right|_{\max} \tag{23}$$

where h is the minimum grid spacing.

5.2 Computation of the Lagrange multiplier

The Lagrange multiplier in Eq.(21) needs to be determined such that the constraint remains feasible or least moves towards the feasible region. A new technique for computing the Lagrange multiplier for the level set method is introduced and is presented for a general problem in the form:

$$\text{Minimize}: \; A(u) = B(u) + \lambda G(u) \tag{24}$$

where $A(u)$ is the Lagrangian function, $B(u)$ is the original objective and $G(u)$ is the constraint. The shape sensitivity of the general problem is:

$$A'(u) = \int_{\Gamma_0} (s_b + \lambda s_g) V_n d\Gamma_0 \tag{25}$$

where s_b and s_g are sensitivities for the objective and constraint, respectively. The change in the constraint, ΔG during an update of the implicit function can be estimated by evaluating the following integral:

$$\Delta G(\lambda) \approx \Delta t \int_{\Gamma_0} s_g V_n(\lambda) d\Gamma_o \tag{26}$$

where V_n can be defined using Eq.(25). Therefore, the velocity function is a function of the Lagrange multiplier. The integral in Eq.(26) can be evaluated numerically for a trial value of λ:

$$\Delta G(\lambda) \approx \Delta t \sum_{i=1}^{m} s_{g,i} V_{n,i}(\lambda) |\Gamma_i| \tag{27}$$

where m is the number of points on the boundary where $V_{n,i}$ is computed and $|\Gamma_i|$ is the boundary surface area associated with point i. Most of the values in Eq.(27) only need to be computed once during an iteration of the optimization, as only the velocity function values change with λ. This leads to an efficient scheme for estimating the change in the constraint for a given value of λ. Equation (27) was used with Newton's method to compute the required value of the Lagrange multiplier for a target value of ΔG.

If the constraint is linear then Eq.(26) is a good approximation for the change in the constraint. However, for non-linear constraints the error in the estimate can increase. This error can be reduced if the update step size, Δt is small. Therefore, the proposed approach for satisfying general constraints can limit the efficiency of the level set method, unless the constraints are linear, or approximately linear. In the current level set framework and for the problem studied in this paper, the proposed method works well for satisfying the constraint.

6. Aero-structural analysis

A multidisciplinary approach is required to analyze the aero-structural problem. Three main tools were used: The Doublet Lattice Method (DLM) [17,18] was used to compute the lift force on the wing, the Finite Element Method (FEM) [19] was used to compute the deformed shape of the wing for a given loading and the Finite Plate Spline (FPS) method [20] was used to transfer information between the DLM and FEM. This section details how these tools were used to solve the aero-structural equilibrium equation, Eq.(1), and the adjoint equations, Eqs.(10,15).

6.1 Doublet Lattice Method

The wing planform was divided into discrete boxes each with a control point at the ¾ chord position. The DLM was used to compute the pressure acting on each box for a given distribution of upwash at the control points:

$$Dc_p = w \tag{28}$$

where D is a matrix of non-dimensional aerodynamic influence coefficients, c_p is a vector of box pressure

coefficients and w is the non-dimensional upwash. The DLM can be used to study subsonic unsteady aerodynamics, where each term in Eq.(28) has a complex component. However, in this work only steady aerodynamics were of interest, thus Eq.(28) had only real components. The non-dimensional upwash was by defined as the upwash divided by the free stream velocity, or true airspeed. Thus, for a thin, flat and rigid wing set at an angle of attack, α, the upwash is simply $-\alpha$. For steady aerodynamics, the coefficients in the D matrix are only dependent on the wing planform and Mach number.

6.2 Finite Element Analysis

The wing internal structure was discretized into equal sized eight-node trilinear continuum elements with incompatible modes. Incompatible modes were used to improve the performance of the element in bending [19]. It was assumed that the structure was made from an isotropic, linear-elastic material and that geometric non-linearity from large deflections could be ignored. Thus, for a given load vector the deformed shape of the wing structure was computed by solving:

$$Ku = f \tag{29}$$

The boundary conditions applied to the FEA were to fix all degrees of freedom at the wing root.

6.3 Finite Plate Spline

The FPS method was used to transfer information between the DLM and FEA. The information was transferred through a plate finite element mesh that lies between the DLM and FEA discretizations. Constraints on the FPS mesh were computed at locations that coincide with the DLM box centers and a subset of the FEA nodes. Solving the FPS finite element equation under these constraints allows the formulation of two matrices that relate aerodynamic and structural quantities:

$$f = qSc_p \tag{30}$$

$$w = Tu \tag{31}$$

where S is a matrix that computes the loading on the structure from the pressure coefficients, T is a matrix that computes the upwash due to the deformed wing shape from the structural displacements and q is the dynamic pressure.

In forming the S matrix it was assumed that the pressure acts at the centre of each DLM box and therefore a moment was added due to the offset distance between the box control point and centre. However, these moments get transferred into pure vertical loads through the FPS method. The resulting vertical loads were applied to the upper surface of the wing. The T matrix in Eq.(31) converts pure vertical deflections from the FEA into the upwash components required for the DLM method. To improve the stability of the transformation the vertical deflection of the wing was computed by averaging the deflections of the upper and lower surfaces. This was necessary as the DLM assumes that the wing is a thin plate and cannot account for a through thickness variation in vertical deflection.

Together, S and T are transfer matrices that allow information to pass between the DLM and FEA. They can be used to formulate an aerodynamic stiffness matrix. Substituting Eq.(28) into Eq.(30), then into Eq.(31), yields:

$$f = qSD^{-1}Tu \tag{32}$$

Therefore, the aerodynamic stiffness matrix is:

$$Q = qSD^{-1}T \tag{33}$$

6.4 Solution procedure

The aerodynamic stiffness matrix can be used directly to solve the aero-structural equilibrium equation, Eq.(1). However, Q is a dense matrix and K is sparse. Thus, the methods usually employed to efficiently solve the static linear elastic equation, Eq.(29) may not be efficient for solving the coupled equation. Therefore, it can be more efficient to use an iterative approach to solve the aero-structural equilibrium equation, without explicitly computing the aerodynamic stiffness matrix. The iterative approach employed in this work is outlined below:

1. Set up the transfer matrices S and T using the FPS method.
2. Solve the DLM equation for a fixed angle of attack, Eq.(28) and transform the c_p into f_c using Eq.(30).
3. Solve $Ku = f_c + f_v$ (using initial $f_v = 0$)
4. Transform u into upwash using Eq.(31)
5. Solve Eq.(28) for c_p due to the deformed wing shape.
6. Transform c_p into a new f_v using Eq.(30)
7. If there is a small change in f_v then equilibrium has been reached, otherwise go back to Step 3.

Steps 1 and 2 are only performed once at the start of the optimization, whereas steps 3-7 are performed each iteration. Further efficiency can be gained by setting the initial value of the variable force, f_v to the converged solution from the previous optimization iteration. Also, the D matrix does not change during the optimization. Thus, the inverse or decomposed matrix can be computed once at the start and then used to efficiently solve for the pressure coefficients during step 5.
The iterative approach was also used to solve for the dual responses, but with some modifications, as the aerodynamic stiffness matrix is transposed in Eq.(10) and Eq.(15). From Eq.(33) the transposed matrix is:

$$Q^T = qT^T\left(D^{-1}\right)^T S^T \tag{34}$$

Steps 4-6 are replaced by the following when solving for the adjoint response:

4. Evaluate $S^T p = w$ (pseudo wash)
5. Solve $c_p = (D^{-1})^T w$ (pseudo pressure)
6. Then: $Q^T p = qT^T c_p$ (pseudo variable load)

7. Example
The multidisciplinary topology optimization method for wing internal structure was demonstrated with an example. The example wing was rectangular with no sweep or taper and the domain for the internal structure was for the full span and from the leading edge to 80% of the chord. The details of the example problem are summarized in Table 1.

Table 1: Example problem details.

Parameter	Value
Wing semi-span	6.0 m
Root chord	2.0 m
Structure depth	0.3 m
Angle of attack (α)	5.0º
True airspeed	85 m/s
Air density	1.2 kg/m^3
Mach number	0.25
Fixed (half) aircraft mass	750 kg

The wing structure was made from material with a Young's modulus of 1.0 GPa, Poisson's ratio of 0.33 and density of 500 kg/m^3. The wing structure domain was discretized using elements with an edge length of 0.05 m. Therefore, the FEA mesh was composed of 32 × 60 × 6 elements in the chord, span and through thickness directions, respectively. The upper and lower surfaces of the mesh were constrained to remain part of the structure by fixing the implicit function values for the upper and lower sets of elements. This was necessary to ensure that loading and displacement information could be transferred to and from the FEA, respectively.
For the DLM, the wing planform was divided into 12 × 36 equal sized boxes in the chord and spanwise directions, respectively.
A lattice structure, representing a conventional rib and spar type design, was chosen as the initial design for the wing internal structure, Figure 1. The parameters and initial design were chosen such that the constraint was satisfied..
The wing internal structure obtained from the optimization method is shown in Figure 2 as plan view cross-sections through the thickness. The optimization method removed material from the tip and trailing edge region and reinforced the root and leading edge regions. The optimized design is remarkably different to the more conventional spar-rib type initial design. A comparison of performance characteristics for the optimized and initial design is shown in Table 2.

Figure 1: Wing structure initial design cross-section.

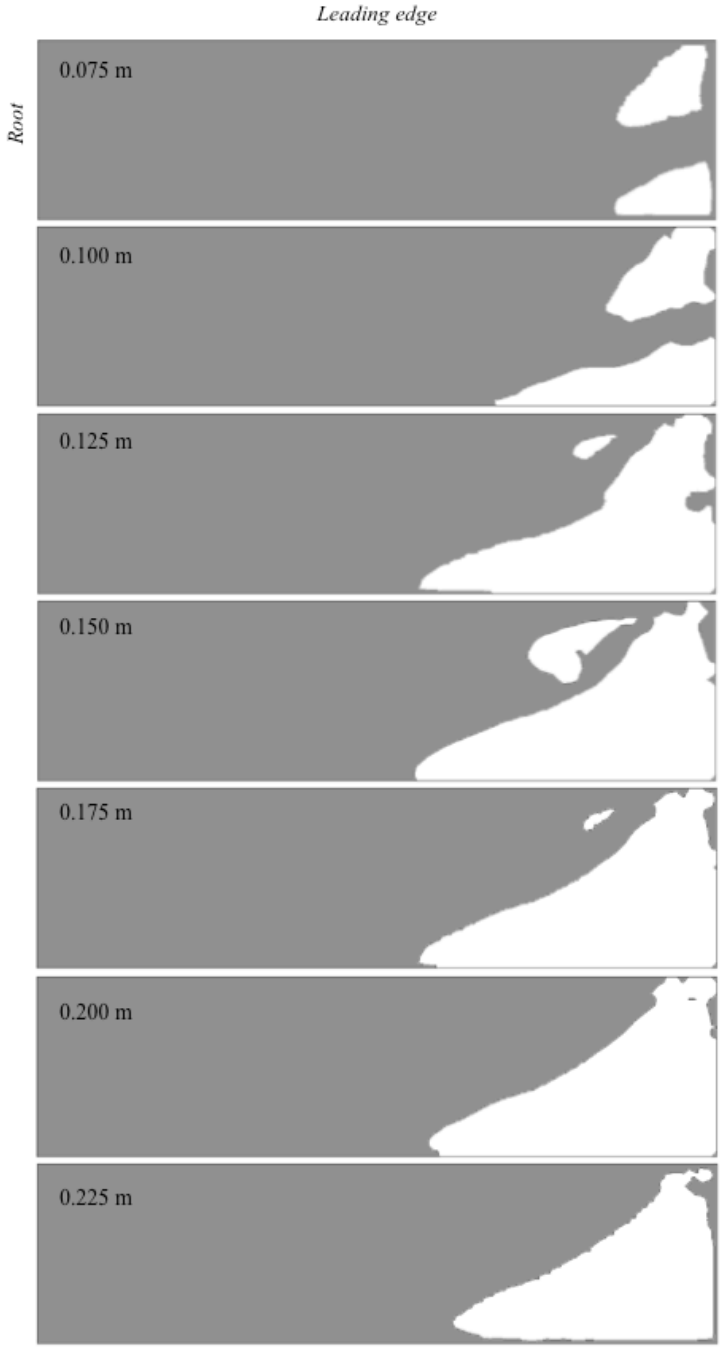

Figure 2: Solution cross-sections through the thickness. The distances indicated are from the lower surface.

Table 2: Comparison of performance characteristics.

Design	Compliance (Nm)	Total Weight (kN)	Total Lift (kN)
Initial	897.1	19.917	19.939
Optimized	870.5	19.882	19.882

The optimized design has lower compliance, weight and hence total lift force, compared with the initial design. This demonstrates that including the design dependent aerodynamic loading, though multidisciplinary analysis and coupled sensitivities, can tailor the stiffness of the wing structure to minimize compliance through both structural reinforcement and load alleviation.

The optimized design converged in 167 iterations and the convergence history is shown in Figure 3. The compliance objective and total lift force deceased monotonically, thus validating the sensitivities derived in Section 4.1. However, the total weight initially increased above the total lift force and the constraint remained violated throughout the optimization until the final iteration. This indicates that the technique used to estimate the change in the constraint and compute the Lagrange multiplier was not accurate enough to enforce the constraint each iteration. However, the technique did move the design towards the feasible region by reducing the total weight until the constraint was satisfied. Therefore, it performed its function over the course of the optimization and a feasible design was obtained.

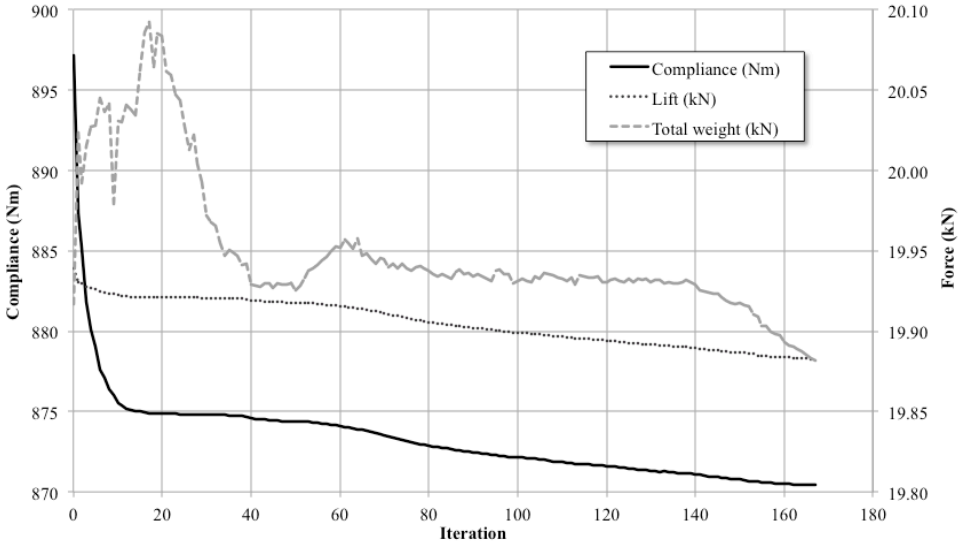

Figure 3: Convergence history for example wing.

The estimate for constraint change is good if the constraint is linear. This may be attributed to the use of a linear time integration scheme when solving the level set update equation, Eq.(20). The total weight part of the constraint is linear by nature. Thus, the results indicate that the lift part of the constraint in non-linear. The estimate for change in lift may be more accurate if a higher order time integration scheme were used. However, this approach would likely add computational cost.

8. Conclusions

This paper introduced a method for optimizing the three-dimensional topology of the internal structure of a wing using the level set method that explicitly included the effect of the coupled aerodynamic loading. The design problem was to minimize the compliance of the structure subject to a constraint that lift must be greater than or equal to weight. A multidisciplinary approach was used to analyze the coupled aero-structural system. Analytical shape sensitivities were derived for compliance and lift that included the effect of the design dependent loading. A new technique was introduced to handle the constraint within the level set based optimization method. This involved approximating the constraint to be linear and then estimating the change using numerical integration. The optimization method performed well, as the structural performance improved and the constraint was satisfied. The compliance was reduced through tailoring the stiffness for both structural reinforcement and load alleviation. The optimized design for an example wing was remarkably different to a conventional wing structure.

9. Acknowledgements
The authors would like to thank Bret Stanford for his advise and validation examples and Max Blair for his example DLM code. This work was partly funded by NASA's Fixed Wing Project under the Fundamental Aeronautics Program.

10. References

[1] V.O. Balabanov and R.T. Haftka, Topology optimization of transport wing internal structure, *Journal of Aircraft*, 33(1), 232-233, 1996.
[2] H.A. Eschenauer and N. Olhoff, Topology optimization of continuum structures: a review, *Applied Mechanics Reviews,* 54(4), 331-390, 2001.
[3] K Maute, and M. Allen, Conceptual design of aeroelastic structures by topology optimization, *Structural and Multidisciplinary Optimization*, 27(1), 27-42, 2004.
[4] B. Stanford and P. Ifju, Aeroelastic topology optimization of membrane structures for micro air vehicles, *Structural and Multidisciplinary Optimization*, 38(3), 301-316, 2009.
[5] B. Stanford and P. Beran, Optimal structural topology of a platelike wing for subsonic aeroelastic stability, *Journal of Aircraft*, 48(4), 1193-1203, 2011.
[6] D.M. De Leon, C.E. de Souza, J.S.O. Fonseca and R.G.A. da Silva, Aeroelastic tailoring using fiber orientation and topology optimization, *Structural and Multidisciplinary Optimization*, 46(5), 663-677,2012.
[7] M.H. Kobayashi, H.T.C. Pedro, R.M. Kolonay, and G.W. Reich, On a Cellular Division Method for Aircraft Structural Design, *The Aeronautical Journal*, 113(1150), 821-831, 2009.
[8] G. Allaire, F. Jouve and A. Toader, Structural optimization using sensitivity analysis and a level-set method, *Journal of Computational Physics*, 194(1), 363–393, 2004.
[9] M.Y Wang, X. Wang and D. Guo, A level set method for structural topology optimization, *Computer Methods In Applied Mechanics and Engineering*, 192(1-2), 227–246, 2003.
[10] P.D. Dunning and H.A. Kim, A new hole insertion method for level set based structural topology optimization, *International Journal for Numerical Methods in Engineering*, 93(1), 118-134, 2013.
[11] A.A. Gomes and A. Suleman, Topology optimization of a reinforced wing box for enhanced roll maneuvers, *AIAA Journal*, 46(3), 548-556, 2008.
[12] C.J. Brampton H.A. Kim and J.L. Cunningham, Level set topology optimisation of aircraft wing considering aerostructural interaction, *14th AIAA/ISSMO Multidisciplinary Analysis and Optimization*, Indianapolis, IN USA, Sep 2012.
[13] C.J. Brampton H.A. Kim and J.L. Cunningham, Algorithm to maintain linear element in 3D level set topology optimization, *ICPRAM 2012 - Proceedings of the 1st International Conference on Pattern Recognition Applications and Methods*, 341-350, 2012.
[14] P.D. Dunning, H.A. Kim and G. Mullineux, Investigation and improvement of sensitivity computation using the area-fraction weighted fixed grid FEM and structural optimization, *Finite Elements in Analysis and Design*, 47(8), 933-941, 2011.
[15] J. Sethian, *Level set methods and fast marching methods*, 2nd ed., Cambridge University Press, New York, 1999.
[16] G. Jiang and D. Peng, Weighted ENO schemes for Hamilton-Jacobi equations, S*iam Journal On Scientific Computing*, 21(6), 2126-2143, 2000.
[17] M. Blair, *A Compilation of the mathematics leading to the doublet lattice method*, Report No. WL-TR-92-3028, Wright laboratory, Wright-Patterson Air Force Base, Ohio, 1992.
[18] W.P. Rodden, P.F. Taylor and S.C McIntosh Jr., Further Refinement of the Subsonic Doublet-Lattice Method, *Journal of Aircraft*, 35(5), 720-727, 1998.
[19] R.D. Cook, D.S. Malkus, M.E. Plesha and R.J. Witt. *Concepts and applications of finite element analysis*, 4th ed., John Wiley & Sons Inc. United States, 2002.
[20] K. Appa, Finite-Surface Spline, *Journal of Aircraft*, 26(5), 495-496, 1989.